PLOS ONE

RESEARCH ARTICLE

Histological, immunohistochemical and transcriptomic characterization of human tracheoesophageal fistulas

Erwin Brosens[1]*, Janine F. Felix[2,3], Anne Boerema-de Munck[2,4], Elisabeth M. de Jong[1,2], Elisabeth M. Lodder[1,5], Sigrid Swagemakers[6,7], Marjon Buscop-van Kempen[2,4], Ronald R. de Krijger[6,8], Rene M. H. Wijnen[2], Wilfred F. J. van IJcken[4], Peter van der Spek[6,7], Annelies de Klein[1], Dick Tibboel[2], Robbert J. Rottier[2,4]

1 Department of Clinical Genetics, Erasmus University Medical Center–Sophia Children's Hospital, Rotterdam, The Netherlands, **2** Department of Pediatric Surgery, Erasmus University Medical Center–Sophia Children's Hospital, Rotterdam, The Netherlands, **3** Department of Pediatrics and Generation R Study Group, Erasmus University Medical Center–Sophia Children's Hospital, Rotterdam, The Netherlands, **4** Department of Cell Biology, Erasmus University Medical Center Rotterdam, Rotterdam, The Netherlands, **5** Department of Clinical and Experimental Cardiology, Heart Center, Academic Medical Center, Amsterdam, The Netherlands, **6** Department of Pathology, Erasmus University Medical Center Rotterdam, Rotterdam, The Netherlands, **7** Department of Clinical Bioinformatics, Erasmus University Medical Center Rotterdam, Rotterdam, The Netherlands, **8** Dept. of Pathology, University Medical Center Utrecht, Utrecht, The Netherlands

* e.brosens@erasmusmc.nl

OPEN ACCESS

Citation: Brosens E, Felix JF, Boerema-de Munck A, de Jong EM, Lodder EM, Swagemakers S, et al. (2020) Histological, immunohistochemical and transcriptomic characterization of human tracheoesophageal fistulas. PLoS ONE 15(11): e0242167. https://doi.org/10.1371/journal.pone.0242167

Editor: David D. Roberts, National Institutes of Health, UNITED STATES

Received: June 5, 2020

Accepted: October 27, 2020

Published: November 17, 2020

Peer Review History: PLOS recognizes the benefits of transparency in the peer review process; therefore, we enable the publication of all of the content of peer review and author responses alongside final, published articles. The editorial history of this article is available here: https://doi.org/10.1371/journal.pone.0242167

Data Availability Statement: Raw data is uploaded to the Gene Expression Omnibus (https://www.

Abstract

Esophageal atresia (EA) and tracheoesophageal fistula (TEF) are relatively frequently occurring foregut malformations. EA/TEF is thought to have a strong genetic component. Not much is known regarding the biological processes disturbed or which cell type is affected in patients. This hampers the detection of the responsible culprits (genetic or environmental) for the origin of these congenital anatomical malformations. Therefore, we examined gene expression patterns in the TEF and compared them to the patterns in esophageal, tracheal and lung control samples. We studied tissue organization and key proteins using immunohistochemistry. There were clear differences between TEF and control samples. Based on the number of differentially expressed genes as well as histological characteristics, TEFs were most similar to normal esophagus. The BMP-signaling pathway, actin cytoskeleton and extracellular matrix pathways are downregulated in TEF. Genes involved in smooth muscle contraction are overexpressed in TEF compared to esophagus as well as trachea. These enriched pathways indicate myofibroblast activated fibrosis. TEF represents a specific tissue type with large contributions of intestinal smooth muscle cells and neurons. All major cell types present in esophagus are present—albeit often structurally disorganized—in TEF, indicating that its etiology should not be sought in cell fate specification.

ncbi.nlm.nih.gov/geo/) with accession number GSE148247.

Funding: This work was supported by the Edgar Doncker Foundation [DT; J.F.F.] and the Sophia Foundation for Scientific Research [Grant Numbers 493 [DT; ADK; E.M.de J.], 436 [A.de M.] and S13-09 [DT; ADK; E.B.] The funders had no role in study design, data collection and analysis, decision to publish, or preparation of the manuscript.

Competing interests: None of the authors have financial, professional, or personal conflicts of interest, all authors reviewed and approved the final manuscript.

Introduction

Esophageal atresia (EA) and tracheoesophageal fistula (TEF) are frequently occurring foregut malformations with an incidence of around 1 in 3,500 births [1–3]. On morphological grounds, five types of esophageal atresia are recognized, of which proximal atresia with a distal TEF is present in 85% of patients [4]. The atresia and TEF are surgically treated in the first days after birth. EA/TEF etiology is likely multifactorial with a strong genetic component [5, 6] and can be either an isolated congenital anatomical malformation or one of the component features of a (suspected) syndrome [7, 8]. Environmental factors have been suggested to play a role in the etiology of EA/TEF, although no single external factor has consistently been identified [3, 9–23]. The genetic etiology of isolated EA/TEF is largely unknown. Approximately 10% of patients with syndromal EA/TEF have chromosomal anomalies, mostly trisomies [1, 24, 25], deleterious Copy Number Variations (CNVs) [26–28] or a monogenetic syndrome [29–40]. Animal models support a genetic contribution [41–63], although, there is little overlap between genes implicated by animal models and the genes known to be involved in human disease [64]. Identification of genetic factors in patients is hampered by the large genetic and phenotypic heterogeneity, insufficient knowledge of disturbed biological processes, gene networks and initial cell type(s) affected. Even the exact mechanisms of normal development of the human foregut and its role in the etiology of EA/TEF are subject of discussion in the literature [65–72].

Up to now, there are only few molecular studies involving human TEF material, which often included small numbers of patients [73–75], and the results are contradictory. Histological studies of TEF and distal esophagus show a mixed contribution of different cell types. Human samples have been described to have (pseudo-) stratified squamous epithelium, tracheobronchial remnants, abnormal mucous glands, a disorganized muscular coat and cartilage [73, 76, 77], but ciliated epithelium has also been observed [77]. Using an unbiased approach, complemented with immunohistochemistry and RT-PCR, the expression of specific proteins and genes in the TEF has been studied in both animals and humans. These include NK2 Homeobox 1 (NKX2-1), Sonic HedgeHog (SHH) and members of the Bone Morphogenic protein (BMP) pathway [73–75, 78–80]. Most of these experiments seem to support a respiratory origin of the TEF in humans, but the number of human TEFs examined was small, ranging from one to nine. In a relatively recent study Smigiel et al. studied the expression pattern of 26 esophageal lower pouches and found enrichment of differentially expressed genes in Wingless and Int- (WNT), SHH and cytokine/chemokine signaling pathways [81].

To gain more insight in the origin of the TEF, we aimed to examine and describe TEF composition using a combination of whole-genome transcription profiling and (immuno-) histochemistry (see S1 Graphical abstract). We hypothesized that such characterization of human TEFs provides insight in the molecular and mechanistic etiology of EA/TEF.

Materials and methods

Human patient control sample characteristics

The protocol for this study was approved by the Medical Ethics Committee of the Erasmus MC Rotterdam, the Netherlands and the Dr. Behcet Uz Children's Hospital in Izmir, Turkey. Written (parental) consent was obtained. This study has been approved by the Erasmus University Medical Center's local ethics board (protocol no.193.948/2000/159, addendum Nos. 1 and 2.) After parental informed consent was obtained, tissue samples of the TEF of children with EA with a distal TEF were taken during primary operative repair of the EA/TEF. The operating surgeons, who have not been involved in the study, determined the safety and technical feasibility of removing the tissue.

We obtained 21 surgically resected tissue samples that were qualitatively suitable for transcriptome profiling. Patient characteristics including sex, gestational age, birthweight and associated anomalies are described in Table 1. All patients were term, except for 1, who was born at 32 weeks. The time of repair was between 2 and 16 days after birth with a median of 2 days. Previously, deleterious variation in the disease genes (*SOX2*, *CHD7*, *MID1*, *SALL1*, *MYCN*, *EFTUD2*, and the *FANC* genes) candidate genes has been determined in patients of which sufficient DNA material was available. Variants have either been determined with a Molecular Inversion Probe (MIP) gene panel [82], Sanger sequencing or Whole Exome Sequencing (WES) during routine diagnostic procedures. We did not have sufficient DNA of patient 3, 23 and 28. Moreover the Copy number profiles of all patients except patient 3 and 18 were determined previously [26]. Several patients had a rare CNV of uncertain significance. Patient SKZ_0106 was diagnosed with CHARGE syndrome. No other causal mutations were identified in these patients. Furthermore, three tracheal, three esophageal and four lung samples were selected to serve as control tissues. Control tissue (lung, trachea and esophagus) was received from the tissue bank of the Erasmus MC. Control samples were taken from autopsies of children of 17–25 weeks gestational age who had died of causes not related to trachea, esophagus or lung abnormalities and in whom there was no reason to assume any abnormalities of these organs.

Table 1. Patient characteristics.

Patient	Gender	GA (wk+d)	BW (g)	IUGR	TSD	*Outcome*	*Associated anomalies*						*Genetic anomalies*
							V	A	C	R	L	Other	
SKZ_0399	M	38+4	3825	-	1	Alive	-	+	-	-	+	A, B, D, E	Gain chr12:74018363–74108097 hg19
SKZ_0401	M	34+1	2060	-	3	Alive	-	-	+	-	-	-	
SKZ_1032	M	37+4	2640	-	2	Alive	-	-	+	-	-	-	
SKZ_0106	F	34+6	1200	+	3	Deceased	-	-	-	-	-		CHARGE syndrome
SKZ_0150	F	38+0	2800	-	2	Alive	-	-	+	-	+	-	
SKZ_0416	F	33+5	1750	-	1	Alive	-	-	-	+	-	B	Gain chr8:66955527–66980813 hg19 (*de novo*)
SKZ_0286	M	35+6	1780	+	2	Alive	-	-	+	+	-	A	
SKZ_1344	M	42+0	3810	-	1	Alive	-	-	-	-	-	A, B	
SKZ_1003	M	37+2	3375	-	2	Alive	+	-	-	-	-	C	Loss chr14:38928454–39044917 hg19
SKZ_1470	M	31+2	1780	-	1	Alive	-	-	-	-	-	-	
SKZ_1150	F	36+2	2120	-	2	Alive	-	-	+	-	-	-	
SKZ_0845	F	41+5	3170	-	2	Alive	+	-	-	-	-	D	Loss chr12:74018363–74108097 hg19
SKZ_0123	M	37+1	2865	-	2	Alive	-	-	-	+	-	-	Loss chr3: 8,975,742–9,024,521 h19 Gain chr16:56,937,855–57,151,796 hg19
SKZ_1248	F	37+5	2235	+	1	Alive	-	-	-	-	-	-	Gain chr1:238656294–238780616 hg19 Loss chr10:19498889–20047506 hg19
SKZ_0703	M	42+3	3800	-	1	Deceased	+	-	+	-	-	-	Gain chr3:1813064–2150011 hg19
SKZ_0673	M	40+2	3595	-	0	Alive	+	-	-	-	-	A, B	
SKZ_1466	F	41+0	3775	-	1	Alive	-	-	-	-	-	-	
SKZ_0546	F	40+5	3570	-	1	Alive	-	-	-	+	-	-	
SKZ_1037	M	40+4	3180	-	1	Alive	+	-	-	+	-	-	
SKZ_0720	M	40+1	3615	-	2	Alive	-	-	-	-	-	-	
SKZ_0876	M	36+1	1800	+	1	Deceased	-	+	+	+	-	A, F	

V: Vertebral/Rib; A: Anal; C: Cardiac; R: Renal; L: upper Limb; TSD: Time to surgery in days; F: female; M: male; GA: gestational age; wk: weeks; d: days; BW: birth weight; g: grams; IUGR: intra-uterine growth retardation; Time to surgery: time between birth and surgery; A: single umbilical artery; B: dysmorphic features (mild in patient no.1, 6 and 8); C: cleft lip, jaw and palate; D: toe anomalies; E: hypospadias; F: duodenal atresia; CHARGE: Coloboma, Heart defects, Atresia of choanae, Retardation, Genital anomalies, Ear anomalies.

https://doi.org/10.1371/journal.pone.0242167.t001

In addition to these 21 patient samples, TEF material of 8 patients was available for histological staining. Control samples were paraffin-embedded samples of normal esophagus and trachea from autopsies of children born at term, who had died of unrelated causes. Also, control samples from preterm trachea and esophagus (gestational ages: 19 weeks+6 days and 17 weeks+3 days) were included, from individuals with normal overall development and without thoracic congenital anomalies. This material was obtained from the pathology department of the Erasmus MC in Rotterdam, the Netherlands.

Transcriptome profiling

RNA isolation and quality control. All samples were snap frozen in liquid nitrogen and stored at −80˚C until further processing. Patient and control samples were homogenized on ice in TRIzol reagent (Invitrogen life technologies, Carlsbad, CA, USA) and total RNA was isolated following the manufacturer's instructions, but the organic extraction was repeated by adding 200μl of 0.1% DEPC water to increase RNA yield. RNA was purified using the Rneasy MinElute Cleanup kit (Qiagen, Valencia, CA, USA) and stored at −80˚C until further processing. RNA concentrations and OD 260/280 nm ratios were measured using the NanoDrop® ND-1000 UV-VIS spectrophotometer (NanoDrop Technologies, Wilmington, USA). RNA quality was evaluated by inspecting ribosomal 28S and 18S peaks and using the bioanalyzer (RNA integrity number (RIN) values above 8.0) Samples with low RNA quality were excluded from the transcriptome study.

Depending on the availability and/or quality of purified total RNA, cDNA was synthesized from 0.8–15 μg RNA using the GeneChip Expression 3'-Amplification.

Reagents One-Cycle cDNA Synthesis kit (Affymetrix, Santa Clara, CA, USA). Biotin-labelled cRNA synthesis, purification and fragmentation were performed according to standard protocols. Fragmented biotinylated cRNA was subsequently hybridized onto Affymetrix Human Genome U133 Plus 2.0 microarray chips, which were scanned with the Affymetrix GeneChip Scanner.

Data processing and normalization. The measured intensity values were analyzed using GeneChip Operating Software (GCOS). The percentage of present calls, background, and ratio of actin and GAPDH 3' to 5' indicated a high quality of samples and an overall comparability. Probe sets that were not present (according to Affymetrix MAS5.0 software) in any of the Genechips were omitted from further analysis. Raw intensities of the remaining probe set of each chip were log2 transformed and raw expression values were quantile normalized and transformed back to normal intensity values. Data analysis was carried out using BRB-array tools version 4.6.0 (October 2018) in combination with R version 3.5.1 (July 2018). For each probe set, the geometric mean of the hybridization intensities of all samples was calculated. The level of expression of each probe set was determined relative to this geometric mean and logarithmically transformed (on a base 2 scale) to ascribe equal weight to gene-expression levels with similar relative distances to the geometric mean. Raw data is uploaded to the Gene Expression Omnibus (https://www.ncbi.nlm.nih.gov/geo/; GSE148247. We used the algorithm embedded in the Ingenuity Pathway Analysis tool to infer enriched pathways Analysis settings and thresholds are provided in the supplementary methods.

Class comparison of tissues types. Genes whose expression differed by at least 1.5-fold from the median in at least 7% of the arrays were included in the analysis. Differential gene expression was determined among the classes (1) Esophagus, (2) TEF, (3) Lung, (4) Trachea and (5) all control tissues combined using a random-variance t-test (RV t-test). Genes were considered statistically significant if their p value was less than 0.05. Additionally, a global test using a p-value of 0.05 for each permutation (n = 10000) was used to confirm of whether the

expression profiles differed between the classes by permuting the labels of which arrays corresponded to which classes. Genes passing the individual tissue type comparison random-variance t-tests used to determine the number of differentially expressed genes between each class.

Hematoxylin and eosin staining. Samples were fixed in 10% buffered formaldehyde for two hours and after routine procedures embedded in paraffin. All paraffin blocks were cut into 4 μm sections.

Sections were deparaffinized in xylene and rehydrated. Routine hematoxylin and eosin staining were done and the sections were evaluated for different cell types and general structure of the tissue. Due to a limited amount of material, not all staining could be done on all samples.

Immunohistochemistry

Sections were deparaffinized in xylene and rehydrated in ethanol. Antibody details are shown in S10 File. Endogenous peroxidase was blocked by 3% H_2O_2 in PBS for 20 minutes. For all proteins except SOX2, antigen retrieval was performed by heat induced epitope retrieval in a Tris/EDTA buffer (pH 9.0) for 20 minutes. Antigen-antibody complexes were visualized by a peroxidase-conjugated polymer DAB detection system (ChemMate DAKO Envision detection kit, Peroxidase/DAB, Rabbit/Mouse; Dako, Glostrup, Denmark). Immunohistochemistry for SOX2 was carried out using the Envision+ System (Dako, Glostrup, Denmark) and HRP-DAB colorimetric detection. Antigen unmasking was performed with microwave treatment in 10 mM citric acid buffer (pH adjusted to 6.0, 15 min at 600 W). Staining intensity was classified as negative and positive. Known positive tissues were used as controls. Due to a limited amount of material, not all staining could be done on all samples.

Results

Transcriptome analysis: Whole transcriptome comparison

We compared the transcriptomes of 21 TEFs to 3 esophageal, 3 tracheal and 4 lung samples. Unsupervised hierarchical clustering of all samples showed that TEF differ from the control samples (lung, trachea and esophagus) based on their whole genome transcription profiles (S1A in S1 File). All TEFs clearly clustered together separately from lung and tracheal tissue. Whereas the lung tissue samples also clustered separately, esophageal and tracheal tissue showed more mixed patterns. We compared the expression patterns of these control tissues individually to the TEF. These TEF mostly resembled esophagus based on the lowest number of differentially expressed genes (S1B in S1 File) between TEF and esophagus. The most differentially expressed genes (top 10) when comparing esophagus to TEF and when comparing trachea to TEF are depicted in Table 2, the 50 most differentially expressed genes are depicted in S1C in S1 File (esophagus vs. TEF) and S1D in S1 File (trachea vs TEF). We determined if sex was a biological variable and compared the transcriptomes of male (n = 13) and female (n = 8) TEF (FDR corrected, Foldchange >1.5). Apart from chromosome Y expressed genes (n = 10, S1E in S1 File) there were no differences.

Transcriptome analysis: Pathway enrichment analysis

We studied the enrichment of pathways by the differentially expressed genes (n = 1045, at FDR p-value 0.01) when comparing the human TEF to esophageal and tracheal controls (S11 File). Pathways affected ($p<0.05$, Z-score of the direction change of the pathway at least +/- 1.5) are often related to cell adhesion and the extracellular matrix, the actin cytoskeleton, neuronal development and smooth muscle cell functioning (Table 3). In total, 28 genes were not

Table 2. Top10 differential expressed genes.

Rank E vs TEF	Symbol	Fold change	TEF	E	T	L	Name	EntrezID
1	KCNMB1	-16.888	1719.36	101.81	141.73	80.43	potassium calcium-activated channel subfamily M regulatory beta subunit 1	3779
2	SYNM	-19.903	5323.59	267.48	178.14	144.79	synemin	23336
3	FAM83D	-10.988	698.96	63.61	91.31	81.83	family with sequence similarity 83 member D	81610
4	CNN1	-40.469	6108.81	150.95	233.83	124.38	calponin 1	1264
5	SYNPO2	-30.756	3708.21	120.57	118.79	40.65	synaptopodin 2	171024
6	PLN	-22.613	1017.83	45.01	165.66	73.64	phospholamban	5350
7	MBNL1-AS1	-26.083	768.68	29.47	35.52	21.29	MBNL1 antisense RNA 1	401093
8	CSRP1	-4.806	5547.58	1154.23	878.38	972.03	cysteine and glycine rich protein 1	1465
9	SMTN	-12.793	1616.07	126.32	157.95	160.03	smoothelin	6525
10	LMOD1	-16.01	1156.59	72.24	58.12	27.13	leiomodin 1	25802
1	ACTG2	-9.879	12547.21	975.48	1270.12	604.38	actin, gamma 2, smooth muscle, enteric	72
2	CNN1	-26.125	6108.81	150.95	233.83	124.38	calponin 1	1264
3	ASB2	-19.324	193.24	35.64	10	12.34	ankyrin repeat and SOCS box containing 2	51676
4	SYNM	-29.884	5323.59	267.48	178.14	144.79	synemin	23336
5	DES	-51.004	3623.3	136.06	71.04	51.99	desmin	1674
6	TPM2	-8.798	8613.55	994.58	979.01	557.9	tropomyosin 2	7169
7	SYNPO2	-31.217	3708.21	120.57	118.79	40.65	synaptopodin 2	171024
8	SLC26A7	21.765	13.06	283.76	284.25	54.38	solute carrier family 26 member 7	115111
9	KCNMB1	-12.131	1719.36	101.81	141.73	80.43	potassium calcium-activated channel subfamily M regulatory beta subunit 1	3779
10	HACD1	-13.187	751.91	181.48	57.02	83.98	3-hydroxyacyl-CoA dehydratase 1	9200

Depicted are the geometric measures of intensity (GMI) the expression signatures of the top 10 differentially expressed genes between Esophagus and TEF and the top 10 differentially expressed genes between Trachea and TEF. Genes are ranked on their pairwise parametric P-value, which were all below 0.0000001. The GMI intensity boxes are labeled in a color scale from orange (low) to blue (high). Statistical analysis was done using a multivariate permutation test with a maximum proportion of false discoveries of 0.01, a confidence level of 0.8 1000 permutations. Top 50 genes are depicted in the supplementary data.

https://doi.org/10.1371/journal.pone.0242167.t002

expressed in the control tissues, but were expressed in more than half (n≥11) TEFs (S2A in S2 File). Vice versa, 40 genes were expressed in all controls, but lacked expression in more than half (n≥11) of the TEFs (S2B in S2 File, S13 File) Absence or presence of gene expression could hint at dysregulation of specific genes, pathways or processes. There were no significant biological processes, molecular functions or cellular component enriched in these two gene sets compared to the Homo sapiens reference set.

Transcriptome analysis: Comparison to mouse foregut expression data

We evaluated if genes important for foregut development are differentially expressed between TEF and controls. For this we, used publicly available mouse gene expression data (GSE13040, GSE19873) [83, 84] at different time points (E8.25-E11.5) (S13 File). Indeed, 798 out of the 986 genes with a mouse orthologue gene were also differentially expressed in the mouse foregut across key mouse foregut developmental milestones (E8.5-E11.5) and could be of importance for proper foregut separation. Furthermore, several genes of which animal knockouts develop TEF were differentially expressed between TEF and trachea (Table 4) (MEOX2 downregulation) and between TEF and both trachea and esophagus (FOXF1 upregulation, SOX4 and DYNC2H1 downregulation).

Table 3. Enriched pathways.

	Canonical Pathways	Z score	E vs TEF	Z score	T vs TEF	Remarks
1	Integrin Signaling	-3.000	6.488	-3.000	6.488	ECM, AC
2	HOTAIR Regulatory Pathway	1.789	4.535	0.894	4.535	D
3	Paxillin Signaling	-2.714	4.039	-2.714	4.039	ECM, AC
4	Superpathway of D-myo-inositol (1,4,5)-trisphosphate Metabolism	-1.633	3.386	-1.633	3.386	SMC?
5	TCA Cycle II (Eukaryotic)	-2.449	3.278	-2.449	3.278	E
6	D-myo-inositol (1,4,5)-trisphosphate Degradation	-2.236	3.157	-2.236	3.157	SMC?
7	Calcium Signaling	-2.138	3.015	-1.604	3.015	SMC
8	PTEN Signaling	1.604	2.818	1.604	2.818	D; AP
9	Actin Cytoskeleton Signaling	-1.698	2.717	-1.698	2.717	AC; SMC
10	ERK/MAPK Signaling	-1.886	2.579	-1.414	2.579	D
11	Regulation of Actin-based Motility by Rho	-2.111	2.504	-2.111	2.504	AC; SMC
12	Signaling by Rho Family GTPases	-1.698	2.489	-1.698	2.489	AC; SMC
13	Salvage Pathways of Pyrimidine Ribonucleotides	-1.508	2.398	-1.508	2.398	
14	Ephrin B Signaling	1.890	2.331	1.890	2.331	D
15	Cardiac Hypertrophy Signaling	-2.065	2.243	-1.606	2.243	
16	IGF-1 Signaling	-2.121	2.169	-2.121	2.169	D; e.g. activates 10 and 29
17	BMP signaling pathway	-1.890	1.868	-1.134	1.868	D
18	Actin Nucleation by ARP-WASP Complex	-2.121	1.830	-2.121	1.830	AC; SMC
19	CDK5 Signaling	-0.333	1.643	-1.667	1.643	AC; N
20	Agrin Interactions at Neuromuscular Junction	-2.121	1.609	-2.121	1.609	D; (S)MC; N
21	Thrombin Signaling	-2.111	1.606	-1.508	1.606	
22	Glioma Signaling	-1.667	1.594	-1.000	1.594	
23	Netrin Signaling	-1.890	1.592	-1.890	1.592	N
24	Endocannabinoid Cancer Inhibition Pathway	-2.111	1.571	-2.111	1.571	
25	Gluconeogenesis I	-2.000	1.568	-2.000	1.568	E
26	Apelin Liver Signaling Pathway	2.000	1.568	2.000	1.568	
27	Neuregulin Signaling	-1.890	1.556	-1.890	1.556	N
28	B Cell Receptor Signaling	-1.732	1.416	-1.155	1.416	
29	PI3K/AKT Signaling	-1.508	1.311	-0.905	1.311	D; ECM
30	Regulation of eIF4 and p70S6K Signaling	-1.890	1.307	-1.134	1.307	

Depicted are the canonical pathways at a significance level of 1.3 (-log($p<0.05$)) and a minimum z-score of 1.5 in either directional change of the pathway(n = 30). Pathways are derived by uploading the most significant (FDR, p-value 0.01) differential expressed genes from both the pairwise analysis of TEF vs Esophagus and TEF vs Trachea. E; esophagus, T; trachea, Pathways with functions in ECM; extracellular matrix organization, AC; actin cytoskeleton, D; development, AP; anterior-posterior axis formation, SMC; smooth muscle cell development or functioning, E; energy metabolism, N; neuronal development or functioning.

https://doi.org/10.1371/journal.pone.0242167.t003

Transcriptome analysis: Disease genes and known biological pathways

We determined the expression signatures of syndromal EA genes (n = 114) [64, 85] to see if we could detect differentially expressed genes between tissue types directly related to known genetic actors. One gene was upregulated in all individual TEF samples compared to all other individual esophageal, tracheal and lung controls: the actin binding cytoskeletal protein filamin A (*FLNA*) (Table 4), whilst *FREM2*, *CDH7* and *EFNB2* are downregulated in most individual samples (and differ significantly on a group level). Next, we focused on targeted differential expression analysis of genes from the best described and currently known pathways in human and mouse foregut morphogenesis. This resulted in the identification of 50 genes that were differentially expressed in TEF compared to either lung, trachea and/or

Table 4. (Candidate) disease genes.

Symbol	Parametric P-Value	FDR	Permutation p-value	TEF	E	T	L		EntrezID	Pairwise significant
FLNA	< 1e-07	< 1e-07	< 1e-07	2475.66	342.01	373.05	425.47	filamin A	2316	(E, TEF), (L, TEF), (T, TEF)
FREM2	< 1e-07	< 1e-07	1.00E-04	27.35	*201.78*	*56.96*	*580.9*	FRAS1 related extracellular matrix protein 2	341640	(E, TEF), (E, L), (E, T), (L, TEF), (L, T)
MEOX2	< 1e-07	< 1e-07	< 1e-07	275.68	467.28	827.06	1579.52	mesenchyme homeobox 2	4223	(E, TEF), (E, L), (L, TEF), (T, TEF), (L, T)
FOXF1	< 1e-07	< 1e-07	< 1e-07	632.2	289.48	82.27	*805.29*	forkhead box F1	2294	(E, TEF), (E, L), (E, T), (T, TEF), (L, T)
SOX4	2.00E-07	2.00E-06	< 1e-07	30.98	*125.13*	*164.47*	*190.33*	SRY-box 4	6659	(E, TEF), (L, TEF), (T, TEF)
DYNC2H1	4.00E-07	3.33E-06	< 1e-07	29.98	*64.02*	*83.64*	*136.1*	dynein cytoplasmic 2 heavy chain 1	79659	(E, TEF), (E, L), (L, TEF), (T, TEF)
ROBO2	7.00E-07	5.00E-06	< 1e-07	32.07	*90.24*	*83.42*	*244.19*	roundabout guidance receptor 2	6092	(E, TEF), (E, L), (L, TEF), (T, TEF), (L, T)
FOXC2	2.20E-06	1.38E-05	3.00E-04	57.92	*68.94*	*188.99*	*48.69*	forkhead box C2	2303	(E, T), (T, TEF), (L, T)
TBX5	2.45E-05	0.000136	4.00E-04	228.89	*120.15*	55.34	789.89	T-box 5	6910	(E, L), (L, TEF), (T, TEF), (L, T)
CHD7	9.62E-05	0.000481	1.00E-04	112.55	*239.01*	*170.67*	*220.02*	chromodomain helicase DNA binding protein 7	55636	(E, TEF), (L, TEF), (T, TEF)
COL3A1	0.000221	0.001	0.0011	179.57	676.8	629.91	336.57	collagen type III alpha 1 chain	1281	(E, TEF), (T, TEF)
EFNB2	0.000296	0.00123	0.0015	160.33	*201.78*	277.52	534.77	ephrin B2	1948	(E, L), (L, TEF)
FGFR2	0.000421	0.00162	0.0033	277.79	*342.17*	*232.7*	996.42	fibroblast growth factor receptor 2	2263	(E, L), (L, TEF), (L, T)
HRAS	0.000613	0.00219	0.001	154.97	*107.99*	79.73	68.07	HRas proto-oncogene, GTPase	3265	(L, TEF), (T, TEF)
KIF3A	0.002052	0.00684	0.0016	54.51	*77.26*	93.07	97.43	kinesin family member 3A	11127	(L, TEF), (T, TEF)
SEMA3E	0.002864	0.00895	0.0062	52.25	*34.47*	*14.88*	*113.35*	semaphorin 3E	9723	(E, L), (T, TEF), (L, T)
DACT1	0.004969	0.0146	0.0074	159.64	*180*	390.57	308.14	dishevelled binding antagonist of beta catenin 1	51339	(L, TEF), (T, TEF)
RARA	0.005746	0.016	0.0104	78.7	*82.26*	*244.88*	*18.05*	retinoic acid receptor alpha	5914	(E, L), (L, TEF), (L, T)
FOXC1	0.011795	0.0305	0.023	95.07	*42.1*	208.95	36.94	forkhead box C1	2296	(E, T), (L, TEF), (L, T)
ITGA4	0.012194	0.0305	0.0196	21.71	*24.9*	*48.67*	*56.07*	integrin subunit alpha 4	3676	(L, TEF), (T, TEF)
FOXP2	0.033228	0.0791	0.0447	360.41	158.45	188.3	*308.76*	forkhead box P2	93986	(E, TEF)
NIPBL	0.044314	0.0963	0.0572	84.51	*157.38*	*125.07*	*163.82*	NIPBL, cohesin loading factor	25836	(L, TEF)
CC2D2A	0.046041	0.0963	0.0498	148.68	*107.28*	*184.85*	203.1	coiled-coil and C2 domain containing 2A	57545	(E, L), (E, T)
MYCN	0.04623	0.0963	0.0654	34.47	*58.01*	*59.03*	*84.56*	MYCN proto-oncogene, bHLH transcription factor	4613	(L, TEF)

Depicted are the geometric measures of intensity (GMI) the expression signatures of differentially expressed (candidate-) EA disease genes [64, 85]: (1) Esophagus, (2) TEF, (3) Lung and (4) Trachea. Pairwise significance is depicted in the last column. The GMI intensity boxes are labeled in a color scale from orange (low) to blue (high). For example: Highly upregulated in TEF is the expression of FLNA compared to all control tissue types and downregulated is the expression of MEOX2. Genes are ranked on their pairwise class comparison according to the random variance t-test analysis. The columns are sorted by the parametric P-value, the false discovery rate (FDR) and the univariate permutation p-value.

https://doi.org/10.1371/journal.pone.0242167.t004

esophagus controls and include key factors as *PTCH1*, *BMP2*, R-SMADS, I-SMADS and *SMAD4* (S3 File).

Transcriptome analysis: Expression of cell type specific genes

Using gene sets representative for smooth muscle, enteric neurons, epithelium and chondrocytes we determined if these signatures were also present in TEF. For instance, during human

enteric nervous system development enteric neural crest cells migrate through the foregut (week 4) and arrive in the distal hindgut (week 7) [86]. These cells form the enteric nervous system are critical in the control of smooth muscle cell functioning and intestinal motility [87]. We compared the expression patterns of genes involved in smooth muscle cell functioning, genes crucial in neuronal functioning and markers for neuronal subtypes and enteric neurons and glia specifically between TEF and controls.

Many smooth muscle contraction genes are overexpressed in TEF compared to esophagus as well as trachea (*KCNMB1*, *LMOD1*, *SMTN*, *CNN1*, *MYL9*, *MYOCD*, *ACTG2* and *MYLK*). The overexpression of these genes is likely the result of the large contribution of intestinal SMC in TEF as the smooth muscle enteric form of gamma 2 (*ACTG2*) is strongly upregulated in trachea (Table 2, S1C, S1D in S1 File and S4 File). Moreover, many neuronal genes (e.g. *KCNMB1*, *KCND3*, *KCNMA1*, *CHRM3*, *VIP*), are overexpressed in TEF, indicative of the presence of neurons in TEF. However, genes of the enteric nervous system are either not differentially expressed, or mostly higher in trachea (S5 and S6 Files). The trachea has a pseudostratified ciliated columnar epithelium (marked by high *KRT8* and *KRT18* expression) and the esophagus has a stratified squamous epithelium signature (marked by high *KRT14*, *KRT5*, *KRT1* and *KRT10* expression). TEF has high KRT8 as well as high KRT14 and KRT5, indicating that both ciliated and stratified epithelium might be present (S7 File). The trachea has cartilage rings. We used the cartilage markers described in S8 File, but could not get a clear cartilage signature as genes were differentially expressed across TEF and control tissues.

Histology

TEF material of 8 patients (not evaluated using micro-array) were available for immunohistochemical staining. As expected, the mucosa of the esophagus consisted of squamous epithelium, whereas the trachea displayed ciliated epithelial cells (Fig 1). Hematoxylin (HE) and eosin stained slides showed squamous epithelium in the TEFs (Fig 2). The muscular layer of the TEFs showed variable degrees of disorganization. No cartilage was found in the TEF samples.

Immunohistochemistry

Expression levels of key marker proteins (NKX2-1, BCL-2, MKI-67, RAR-α, RAR-β, SOX-2, BMP2, BMP4, BMPR1A, BMPR1B, BMPR2, Noggin) of foregut development were determined with immuno-histochemical staining. We evaluated if the results of the immunostaining were representative of the results of the transcriptome profiling. All TEF samples were negative for NKX2-1 immunostaining, as were normal trachea and esophagus (Table 5). BMP2 staining was absent in TEF, but positive in preterm and term esophagus and trachea (Fig 3). BMP4 staining was negative in all samples tested. The BMP receptors BMPR1A, BMPR1B and BMPR2 were positive in all samples. There was some RAR-alpha positive staining in term esophagus and TEF (Fig 3). RAR-beta staining was positive in TEFs, especially in the basal epithelium. All control samples were positive, where the trachea stained weakly and the esophagus strongly positive. SOX2 nuclear expression was found throughout the epithelium of the TEFs, with very strong cytoplasmic staining on the luminal side and less strong, but still clearly present, granular staining on the basal side. The control samples all showed cytoplasmic as well as nuclear SOX2 staining. An overview of the results of all stainings can be found in Table 5.

Discussion

In this study we used an unbiased whole transcriptome approach to characterize the TEF in detail in order to get more insight in their etiology. The esophagus and trachea are foregut-

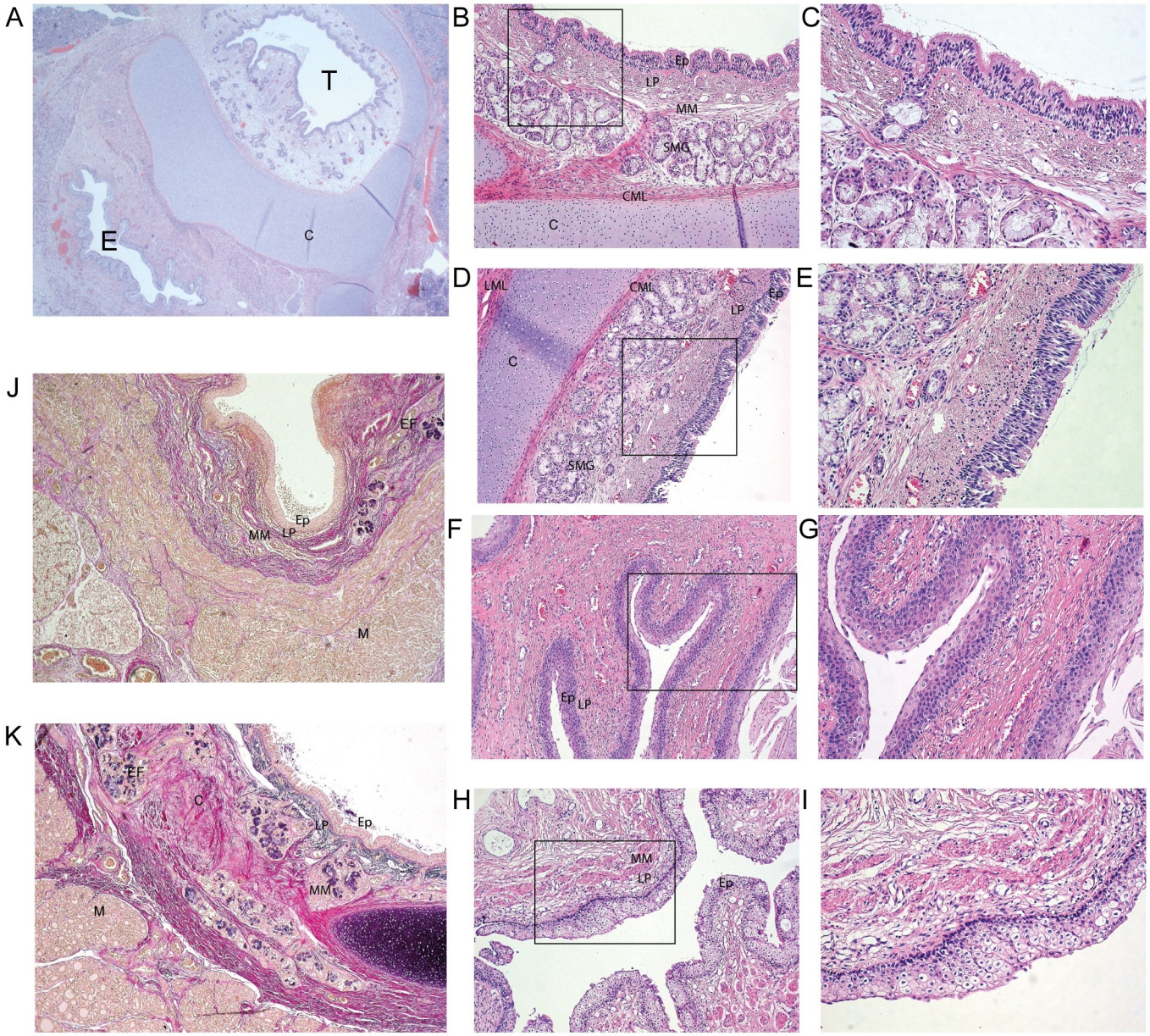

Fig 1. A-E. Hematoxylin and eosin (HE) stained sections of normal esophagus and trachea. A. Cross section of normal esophagus (E) and trachea (T) with surrounding cartilage (C) at 1.25 x magnification. B-C. Overview and detail of normal trachea with multilayered cylindrical epithelium (ep), underlying lamina propria (lp), muscular layer (mm) and seromucinous glands (smg); at the bottom of the image, the circular muscular layer (cml) and underlying cartilage can be seen. (at 10x (left) and 20x (right) magnification) C-D. Overview and detail of normal trachea covered with multilayered cylindrical epithelium (ep), with underlying glands, circular (cml) and longitudinal muscle layer (lml), both next to cartilage. (at 10x (left) and 20x (right) magnification) F-G and H-I. Normal esophagus covered by multilayered squamous epithelium (ep). (at 10x (left) and 20x (right) magnification) J and K. Elastic stain with elastic fibers in black (EF), collagen in pink (COL) and muscle (M) in yellow. In J an overview of normal esophagus is seen, with normal trachea in K. (at 4x magnification).

https://doi.org/10.1371/journal.pone.0242167.g001

derived and during development there is a disturbance resulting in a faulty separation of these two structures. Unsupervised clustering analysis revealed that the most of the TEFs clustered separately from the controls and likely share more characteristics among each other on the level of gene expression than with these control tissues. TEF have large intestinal smooth muscle cell contribution, neuronal genes are expressed and there is likely ciliated and as well as

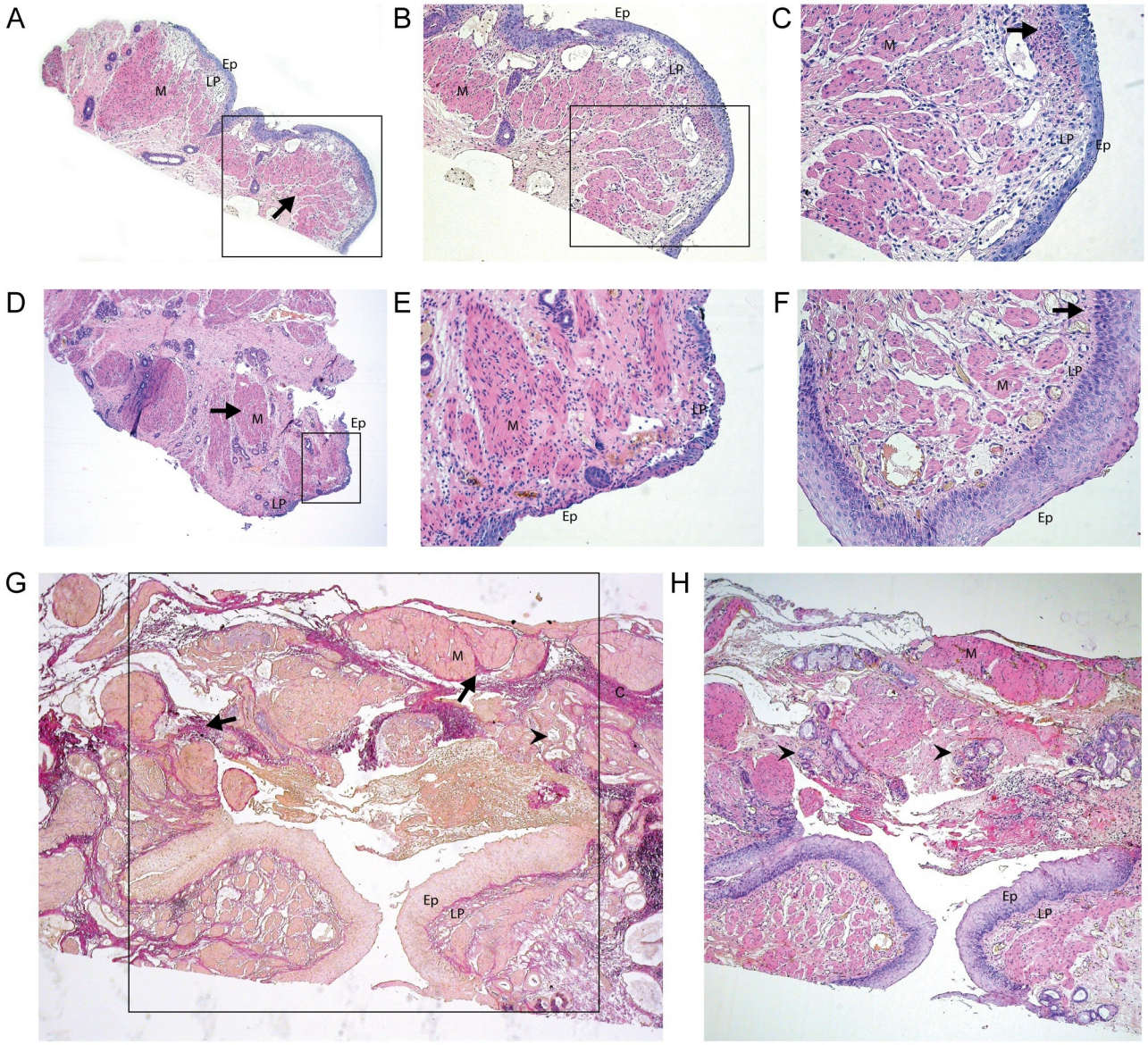

Fig 2. A-D. Overview and details of TEF. TEF walls covered by squamous epithelium (ep), with underlying lamina propria (lp) and muscular layer (m). The muscle layer appears irregular and fragmented in the overview of A-C and D, E and F. In the detail images a mild chronic inflammatory infiltrate can be appreciated. (at 4x, 10x and 40x magnification respectivly) G. Elastic and corresponding HE stain (H) of fistula covered with squamous epithelium, showing disorganized muscle bundles and glandular structures. (at 10x magnification).

https://doi.org/10.1371/journal.pone.0242167.g002

stratified epithelium present. Transcription signatures and histological staining indicate that cell types normally present in esophagus are present in TEF. However, cell layers are often disorganized, which could be due to differences in exposure to signaling molecules. This combined would imply that the etiology of EA/TEF should not be sought in cell fate specification, but perhaps more in those biological processes involved in anterior-posterior or dorsal-ventral axis patterning or defects in signaling from the notochord or mesenchyme.

Two pathways known to be involved in tracheoesophageal development are affected. The first -he BMP pathway [49, 51]—is downregulated. Bone morphogenic proteins as Bmp4 and Bmp7 [49, 88] and their upstream regulator Noggin and Shh regulate dorsoventral patterning

Table 5. Overview of the results of the immunohistochemical staining and differential expression analysis.

	Term esophagus	Preterm esophagus	Term trachea	Preterm trachea	TEF
NKX2-1	-	-	-	-	-
BCL-2	-	+/-	+	+	-
mRNA	N/p	++	N/p	+++	+
(M)Ki-67	+	N/p	+	N/p	+
RAR-α	+/-	-	-	-	+/-
mRNA	N/p	-	N/p	+++	-
RAR-β	+	+	+	+	+
SOX-2	+	+	+	+	+
BMP2	+	+	+	+	-
mRNA	N/p	++	N/p	+	-
BMP4	-	-	-	-	-
BMPR1A	+	+	+	+	+
BMPR1B	+	+	+	+	+
BMPR2	+	+	+	+	+
Noggin	+	+	+	+	+[a]
MMP-14	+/-	N/p	+/-	N/p	+
mRNA	N/p	++	N/p	+++	+
MMP-2	- epi.+ mes.	+/-	+	+	+/- epi.+ mes.
mRNA	N/p	++	N/p	+++	+

-: negative staining; +/-: variable results, some samples positive and some negative; + positive staining (mild); ++ positive staining (moderate); +++ positive staining (strong); N/p: not performed; epi: epithelium; mes: mesenchyme; a Mostly positive (see text for details) BCL2, RARα, and BMP2 were also differentially expressed between preterm esophagus, preterm trachea and TEF on mRNA level in the transcriptome samples. (M)Ki-67; marker of proliferation. BCL-2; apoptosis regulator. NKX2-1 staining were done on all patient samples, on all preterm samples and on four term trachea and esophagus samples. RAR-beta staining was done in all case samples, except for one TEF, in four term esophagus and term trachea samples and in all preterm samples. SOX2 staining was done on all case samples, except for one TEF. Furthermore, SOX2 was done on four term trachea and four term esophagus samples and on all preterm samples.

https://doi.org/10.1371/journal.pone.0242167.t005

between endoderm and mesoderm and separation of the foregut into esophagus and the trachea [89]. We did not detect BMP2 protein expression and several genes of the TGF-β / BMP pathway (e.g. *BMP2*, R-SMADS (*SMAD1* & *SMAD5*) Co-SMAD (*SMAD4*) and I-SMADS (*SMAD6* & *SMAD7*) are downregulated. The second -he Ephrin B pathway—is upregulated in TEF. Ephrin B Signaling is upregulated. In contrast, *EFNB2* itself has the lowest expression when TEF is compared to esophagus, trachea and lung (Table 4). Interestingly, absent expression is related to tracheoesophgeal septation problems as *Efnb2* knockout mice develop TEF [90].

When comparing TEF to esophagus and trachea, we see that several interlinked pathways related to the actin cytoskeleton and adhesion to the extracellular matrix are downregulated in TEF (Table 3): integrins mediate cell adhesion to the ECM, link the ECM to the actin cytoskeleton, activate signal transduction pathways such as receptor tyrosine kinases [91, 92]. Coupling of the ECM to the actin cytoskeleton takes place through complexes of proteins such as integrin, vinculin, filamin and paxillin [93]. Paxillin is a scaffold enabling adhesion and growth factor molecules signaling between the plasma membrane and the actin cytoskeleton [94]. During development, Paxillin is involved in the development of mesoderm derived structures and has been shown to be a transducer of fibronectin signaling [95]. In Xenopus, syndecan-4 is required for fibronectin-1 extracellular matrix assembly, acts upstream of BMP and Wnt/JNK signaling [96] and fibronectin 1 Xenopus have foregut defects. The PI3K/AKT Signaling pathway is also downregulated and is essential for endoderm formation [97]. It regulates the

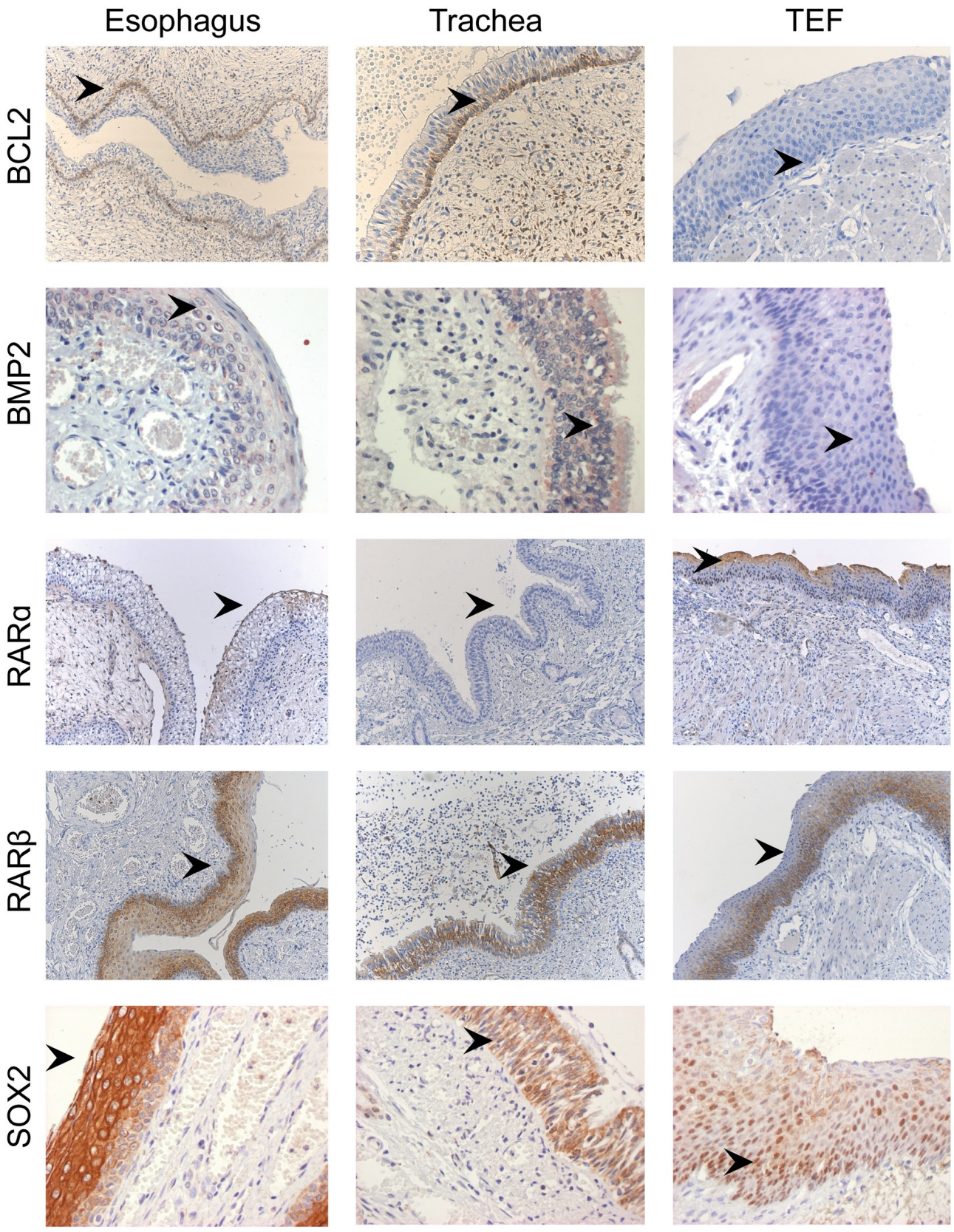
Esophagus
Trachea
TEF
BCL2
BMP2
RARα
RARβ
SOX2

Fig 3. Immunostaining of esophagus, trachea and TEF. The first panel shows presence of bcl2 staining in the basal epithelial cells in both esophagus and trachea, but not in TEF. The second panel shows faint cytoplasmic BMP2 staining in esophagus and trachea, but not in TEF. The third panel shows cytoplasmic retinoic acid receptor alpha (RARα) staining in the upper part of the squamous epithelium of the esophagus and TEF, but not in the cylindrical epithelium of the trachea. In the fourth panel retinoic acid receptor beta (RARβ) shows similar cytoplasmic staining in the lower portion of the epithelium in all three structures. Interestingly, in the lower panel SOX2 shows cytoplasmic staining in esophagus and trachea, while there is evident nuclear labeling of epithelial cells in TEF. BLC2 esophagus and trachea at 10x magnification, TEF at 20x magnification. BMP2 and SOX2 at 40x magnification and RAR-α and RAR-β at 10x magnification.

https://doi.org/10.1371/journal.pone.0242167.g003

levels of fibronectin in the foregut extracellular matrix. Without fibronectin and Integrin alpha 5 the foregut does not fold into a tube [98]. Connected to the extracellular matrix is the actin cytoskeleton. Actin cytoskeleton signaling, actin-based motility and other related pathways are also downregulated. CDK5 signaling is involved in the organization of the cytoskeleton and its contraction in both neurons and muscle [99–102].

Whilst many smooth muscle contraction related genes are upregulated in TEF, calcium signaling and pathways linking the extracellular matrix to the actin filament are downregulated. A process in which these pathways are entwined is myofibroblast directed fibrogenesis in which the actin stress fibers direct extracellular matrix remodelling [103, 104]. In response to TGFB1 fibroblast transform in smooth muscle like cells [105] with upregulation of *ACTA2*, *ACTG2 and* actin associated proteins are induced [106, 107]. BMPR1 activity is required for myoblast activation [108] and the fibrotic gene expression cascade [109] and mediates the abnormal proliferation of vascular smooth muscle cells seen in familial pulmonary arterial hypertension [110]. On transcriptome level, all evidence hints at a disruption of EMC-Cytoskeleton interaction. Immunohistochemistry of genes involved in this signaling cascade (BMPR1A and BMPR1B, MMP2 and MMP4) was not conclusive (Table 5, S10 File).

We performed immunohistochemical staining on some of the most crucial target molecules: e.g. NKX2-1, BMP2, BMP4, Retinoic Acid Receptor (RARα and β) and SOX2. As TEF is mostly derived from preterm infants, we compared TEF to term and preterm control esophagus and trachea. Several genes from the HH, WNT, BMP and retinoic acid signaling pathways remain differentially expressed (S3 File), most of them when comparing TEF to trachea and/or lung. This intriguing observation either indicate that these pathways *remain* disturbed after the original insult resulting in TEF, or indicate that these pathways are *no longer* essential in EA or lung development as TEF biopsies are taken after birth. High *NNKX2.1* and low *SOX2* characterizes future trachea and the opposite is true for future esophagus [111]. Noggin null mice form TEF which are lined with *Nkx2.1* expressing epithelial cells and indicate a respiratory origin [49]. However, *Nkx2.1* expression did not differ between any of the tissue types and TEF (Table 3). NKX2-1 was found by PCR and by immunohistochemistry in the epithelial tubules of the TEFs at term [74]. In rats with Adriamycin-induced EA/TEF, Nkx2.1 was also found by immunohistochemistry in the TEF throughout gestation, although its expression diminished later in pregnancy [78, 79]. The difference between these and our studies may reflect the heterogeneity of the TEFs or timing of developmental stage of controls and TEF.

Based on the theory that TEF originates from the tracheal bifurcation and grows down towards the stomach in a non-branching way, Crowley *et al* studied the expression pattern of *BMP2*, *4* and *7* and *BMPR-IA*, *-IB* and *-II* in normal human lung, trachea and esophagus samples, as well as in samples of the proximal esophageal pouch and the TEF of nine patients with EA/TEF [75]. *BMP*-expression patterns in the proximal pouch were the same as in normal esophagus. The TEF tract showed a mixed pattern, with BMPs being absent (comparable to trachea) and also absence of the BMP-receptors, except for BMPR-II (comparable to esophagus), thereby confirming the hypothesis of an imbalance between ligands and receptors [75] Both mRNA and protein expression (see Table 5) of BMP2 and BMP4 are absent in TEF in

our study. There was no BMP4 protein expression nor is *BMP4* differentially expressed on mRNA level between preterm esophagus, preterm trachea or TEF. The BMPR2 receptor has protein expression throughout the tissues, including TEF. Thus in general, our findings are in line with these previous studies [75].

Two genes from the RA pathway (*ADH1B* and *RETSAT*) are involved in retinol metabolism, but are not crucial proteins involved in retinoic acid signaling. Similar patterns of immunohistochemical staining of these two retinoic acid receptors was observed in the lung, trachea and TEF specimens illustrative of the lack of difference in gene expression of genes involved in retinoic acid signaling. SOX2 is a transcription factor that, depending on its posttranslational status [112], should be predominantly present in the nucleus. Although the involvement of *SOX2* in the development of the foregut in general and EA/TEF in particular has been demonstrated in human and animal studies [37, 46, 49, 113–115], this involvement is not reflected the observed expression patterns of the different tissues in our study as we did not detect differences between TEFs and controls. Further studies, using more quantitative techniques may provide more detailed information on this.

We detect expression of most smooth muscle cell (SMC) contraction related genes (S 4) as well neuronal marker genes (S5 File), and enteric neuron and glia markers [116] (S6 File). There are strong indications that there are cells of the enteric nervous system and smooth muscle cells present in the TEF. As foregut separation occurs after ENCC migrate through the foregut, an ENS signature could be present in TEF. Indeed, the presence of SMC gene expression (e.g. *MYH11*, *MYL9*, *MYLK* and the intestinal specific *ACTG2*), potassium and calcium voltage gated channels (e.g. *KCNMB1*, *CACNA2D1*), neuronal subtype markers (e.g. *VIP*, *NPY*, *PENK*, *CARTP*), receptors (cholinergic, dopaminergic, GABBA) and ENS marker genes (*L1CAM*, *TUBB3*, *UCHL1*, *PRPH*, *ELAV4*, neurofilament and peripherin) further strengthen the evidence for a more intestinal program.

Using micro-array-, we can only determine the relative expression within a mix of patient cells. Further experiments in TEF and esophageal biopsies would benefit from a single cell approach, as this would allow for a detailed characterization and quantification of cell types. For instance, we cannot exclude tracheal SMC and neuronal contributions due to our experimental setup. Using single cell transcriptomics-based approaches we could have determined if *ACTG2* –negative SMC were present. Kishimoto et al. show that smooth muscle cell precursor polarization is the starting point for tracheal tube elongation [117]. The neuronal subtypes of trachea and esophagus mostly overlap, although there are esophageal specific neuronal cells [118]. Interestingly, most smooth muscle cell genes are strongly overexpressed compared to all tissue types hinting at a much larger SMC composition of the TEF biopsies and/or myofibroblast activation.

Several keratins are upregulated in TEF compared to all control tissues. *KRT8* and *KRT18* are markers for columnar epithelial markers, whilst *KRT14* and *KRT5* are expressed in the basal layer of stratified squamous epithelial cells, whilst *KRT1* and *KRT10* are expressed in the suprabasal layers [119]. Other markers for early epithelial differentiation include *Itgb4*, *Itgb6* and *Nt5e* (*Cd73*) [120]. During development there is a transition from columnar to pseudostratified epithelium. This transition is likely controlled by *TP63* [121]. Although we could not detect differential expression of *SOX2*, the upregulation of *NT5E* and *ITGB4* hint at the presence of early transition from basal to suprabasal cells. The esophageal epithelium-specific keratins (*KRT4* and *KRT13*) [122] are highly upregulated compared to the control tissues. Interestingly, we can measure upregulation of basal layer markers *KRT14* and *KRT5* as well as a comparable expression level of *KRT8* in esophagus and TEF. During that time there are also cells expressing both *KRT8* as well as *KRT14* [119]. We could not detect a clear cartilage specific signature in TEF.

This study characterizes the transcriptome of TEF and their histological composition.

We determined the relative gene expression of a mix of cells present in TEF and compared this to preterm esophagus, lung and trachea The number of control samples is low compared to the number of TEF. Including more control samples would allow for a more robust differential expression analysis. Furthermore, TEF are not naturally occurring tissue structures and it is not certain that the expression levels seen in this postnatal "end state" of development are representative of early development. Although all major cell types seem present, it is not certain that these cells would function normally. Future experiments using single cell sequencing would allow for a cell type specific comparison.

Conclusions

Tracheoesophageal fistulas are fibrous tubular structures with large contributions of intestinal smooth muscle cells, mostly resembling the esophagus. TEF tissue layers are often structurally disorganized. We could not detect tracheobronchial remnants neither based on expression profiles nor on histological staining. The BMP-signaling pathway, actin cytoskeleton and extracellular matrix pathways are downregulated compared to esophagus and trachea. Pathways related to myofibroblast activated fibrosis are enriched. Additional experiments are required to determine if upregulation of genes involved in the actin cytoskeleton and smooth muscle cell functioning are related to the disorganized structure of the TEF, myoblast activated fibrosis or abnormal the functioning of these cell types [76, 123]. Furthermore, it is important to examine if these processes are disturbed throughout the esophagus and continue to affect neuromuscular functioning with disturbed esophageal motility as a consequence.

Supporting information

S1 File. Differential expression analysis, clustering and sex differences.
(PDF)

S2 File. TEF defining genes.
(PDF)

S3 File. DEGs in retinol metabolism, WNT-, TGFB- and hedgehog signaling.
(PDF)

S4 File. Smooth muscle contraction gene expression.
(PDF)

S5 File. Neuronal marker genes.
(PDF)

S6 File. DEG ENS markers.
(PDF)

S7 File. DEG epithelial markers.
(PDF)

S8 File. DEG cartilage markers.
(PDF)

S9 File. Details of antibodies used for immunohistochemistry.
(PDF)

S10 File. Immunostainings MMP2, MMP14 and BMPR1A.
(PDF)

S11 File. Causal network analysis using IPA©.
(PDF)

S12 File. TEF specific expression pattern analysis.
(PDF)

S13 File. Overlap with mouse developmental transcriptome.
(PDF)

S1 Graphical abstract. Transcriptome study and histochemistry of tracheoesophageal fistula.
(TIF)

Acknowledgments

The authors would like to thank the pediatric surgeons of the Erasmus MC–Sophia Children's Hospital, Monique Oomen of the Erasmus MC tissue bank, Tom de Vries-Lentsch for making the illustrations and Prof. Dr. Münnever Hösgör of the Dr. Behcet Uz Children's Hospital (Izmir, Turkey) for providing TEF material for (immune-) histological staining.

Author Contributions

Conceptualization: Erwin Brosens, Janine F. Felix, Dick Tibboel, Robbert J. Rottier.

Data curation: Erwin Brosens.

Formal analysis: Erwin Brosens, Anne Boerema-de Munck, Elisabeth M. Lodder, Sigrid Swagemakers.

Funding acquisition: Erwin Brosens, Janine F. Felix, Anne Boerema-de Munck, Elisabeth M. de Jong, Annelies de Klein, Dick Tibboel.

Investigation: Anne Boerema-de Munck, Sigrid Swagemakers, Ronald R. de Krijger.

Methodology: Anne Boerema-de Munck, Elisabeth M. Lodder.

Project administration: Anne Boerema-de Munck, Elisabeth M. de Jong, Marjon Buscop-van Kempen.

Resources: Janine F. Felix, Anne Boerema-de Munck, Elisabeth M. de Jong, Rene M. H. Wijnen.

Software: Erwin Brosens, Sigrid Swagemakers, Wilfred F. J. van IJcken.

Supervision: Dick Tibboel, Robbert J. Rottier.

Validation: Marjon Buscop-van Kempen.

Writing – original draft: Erwin Brosens, Janine F. Felix, Robbert J. Rottier.

Writing – review & editing: Erwin Brosens, Janine F. Felix, Ronald R. de Krijger, Rene M. H. Wijnen, Wilfred F. J. van IJcken, Peter van der Spek, Annelies de Klein, Dick Tibboel, Robbert J. Rottier.

References

1. Depaepe A, Dolk H, Lechat MF. The epidemiology of tracheo-oesophageal fistula and oesophageal atresia in Europe. EUROCAT Working Group. Arch Dis Child. 1993; 68(6):743–8. https://doi.org/10.1136/adc.68.6.743 PMID: 8333763

2. Robert E, Mutchinick O, Mastroiacovo P, Knudsen LB, Daltveit AK, Castilla EE, et al. An international collaborative study of the epidemiology of esophageal atresia or stenosis. Reprod Toxicol. 1993; 7 (5):405–21. https://doi.org/10.1016/0890-6238(93)90085-l PMID: 8274816
3. Torfs CP, Curry CJ, Bateson TF. Population-based study of tracheoesophageal fistula and esophageal atresia. Teratology. 1995; 52(4):220–32. https://doi.org/10.1002/tera.1420520408 PMID: 8838292
4. del Rosario JF, Orenstein SR. Common pediatric esophageal disorders. Gastroenterologist. 1998; 6 (2):104–21. PMID: 9660528
5. Choinitzki V, Zwink N, Bartels E, Baudisch F, Boemers TM, Holscher A, et al. Second study on the recurrence risk of isolated esophageal atresia with or without trachea-esophageal fistula among first-degree relatives: no evidence for increased risk of recurrence of EA/TEF or for malformations of the VATER/VACTERL association spectrum. Birth Defects Res A Clin Mol Teratol. 2013; 97(12):786–91. https://doi.org/10.1002/bdra.23205 PMID: 24307608
6. Schulz AC, Bartels E, Stressig R, Ritgen J, Schmiedeke E, Mattheisen M, et al. Nine new twin pairs with esophageal atresia: a review of the literature and performance of a twin study of the disorder. Birth Defects Res A Clin Mol Teratol. 2012; 94(3):182–6. https://doi.org/10.1002/bdra.22879 PMID: 22287212
7. van Beelen NW, Mous DS, Brosens E, de Klein A, van de Ven CP, Vlot J, et al. Increased incidence of hypertrophic pyloric stenosis in esophageal atresia patients. Eur J Pediatr Surg. 2014; 24(1):20–4. https://doi.org/10.1055/s-0033-1352527 PMID: 23982818
8. Bogs T, Zwink N, Chonitzki V, Holscher A, Boemers TM, Munsterer O, et al. Esophageal Atresia with or without Tracheoesophageal Fistula (EA/TEF): Association of Different EA/TEF Subtypes with Specific Co-occurring Congenital Anomalies and Implications for Diagnostic Workup. Eur J Pediatr Surg. 2018; 28(2):176–82. https://doi.org/10.1055/s-0036-1597946 PMID: 28061520
9. Nora JJ, Nora AH. Birth defects and oral contraceptives. Lancet. 1973; 1(7809):941–2. https://doi.org/10.1016/s0140-6736(73)91398-6 PMID: 4123872
10. Kaufman RL. Birth defects and oral contraceptives. Lancet. 1973; 1(7816):1396. https://doi.org/10.1016/s0140-6736(73)91731-5 PMID: 4122792
11. Nora AH, Nora JJ. A syndrome of multiple congenital anomalies associated with teratogenic exposure. Arch Environ Health. 1975; 30(1):17–21. https://doi.org/10.1080/00039896.1975.10666626 PMID: 1109267
12. Lammer EJ, Cordero JF. Exogenous sex hormone exposure and the risk for major malformations. Jama. 1986; 255(22):3128–32. PMID: 3702023
13. Ramirez A, Espinosa de los Monteros A, Parra A, De Leon B. Esophageal atresia and tracheoesophageal fistula in two infants born to hyperthyroid women receiving methimazole (Tapazol) during pregnancy. Am J Med Genet. 1992; 44(2):200–2. https://doi.org/10.1002/ajmg.1320440216 PMID: 1456292
14. Di Gianantonio E, Schaefer C, Mastroiacovo PP, Cournot MP, Benedicenti F, Reuvers M, et al. Adverse effects of prenatal methimazole exposure. Teratology. 2001; 64(5):262–6. https://doi.org/10.1002/tera.1072 PMID: 11745832
15. Oakley GP Jr., Flynt JW Jr., Falek A. Hormonal pregnancy tests and congenital malformations. Lancet. 1973; 2(7823):256–7.
16. Torfs CP, Milkovich L, van den Berg BJ. The relationship between hormonal pregnancy tests and congenital anomalies: a prospective study. Am J Epidemiol. 1981; 113(5):563–74. https://doi.org/10.1093/oxfordjournals.aje.a113133 PMID: 7194580
17. Czeizel A, Ludanyi I. An aetiological study of the VACTERL-association. Eur J Pediatr. 1985; 144 (4):331–7. https://doi.org/10.1007/BF00441773 PMID: 4076249
18. Rittler M, Paz JE, Castilla EE. VATERL: an epidemiologic analysis of risk factors. Am J Med Genet. 1997; 73(2):162–9. https://doi.org/10.1002/(sici)1096-8628(1997)73:2<162::aid-ajmg10>3.0.co;2-s PMID: 9409866
19. Felix JF, Steegers-Theunissen RP, de Walle HE, de Klein A, Torfs CP, Tibboel D. Esophageal atresia and tracheoesophageal fistula in children of women exposed to diethylstilbestrol in utero. Am J Obstet Gynecol. 2007; 197(1):38 e1–5. https://doi.org/10.1016/j.ajog.2007.02.036 PMID: 17618749
20. Zwink N, Choinitzki V, Baudisch F, Holscher A, Boemers TM, Turial S, et al. Comparison of environmental risk factors for esophageal atresia, anorectal malformations, and the combined phenotype in 263 German families. Diseases of the esophagus: official journal of the International Society for Diseases of the Esophagus. 2016; 29(8):1032–42.

21. Feng Y, Chen R, Li X, Mo X. Environmental factors in the etiology of isolated and nonisolated esophageal atresia in a Chinese population: A case-control study. Birth Defects Res A Clin Mol Teratol. 2016; 106(10):840–6. https://doi.org/10.1002/bdra.23550 PMID: 27494675

22. Wong-Gibbons DL, Romitti PA, Sun L, Moore CA, Reefhuis J, Bell EM, et al. Maternal periconceptional exposure to cigarette smoking and alcohol and esophageal atresia +/- tracheo-esophageal fistula. Birth Defects Res A Clin Mol Teratol. 2008; 82(11):776–84. https://doi.org/10.1002/bdra.20529 PMID: 18985694

23. Michikawa T, Yamazaki S, Ono M, Kuroda T, Nakayama SF, Suda E, et al. Fish consumption in early pregnancy and congenital gastrointestinal tract atresia in the Japan Environment and Children's Study. The British journal of nutrition. 2018:1–9. https://doi.org/10.1017/S0007114518002842 PMID: 30370875

24. Brunner HG, Winter RM. Autosomal dominant inheritance of abnormalities of the hands and feet with short palpebral fissures, variable microcephaly with learning disability, and oesophageal/duodenal atresia. J Med Genet. 1991; 28(6):389–94. https://doi.org/10.1136/jmg.28.6.389 PMID: 1870095

25. Felix JF, Tibboel D, de Klein A. Chromosomal anomalies in the aetiology of oesophageal atresia and tracheo-oesophageal fistula. European journal of medical genetics. 2007; 50(3):163–75. https://doi.org/10.1016/j.ejmg.2006.12.004 PMID: 17336605

26. Brosens E, Marsch F, de Jong EM, Zaveri HP, Hilger AC, Choinitzki VG, et al. Copy number variations in 375 patients with oesophageal atresia and/or tracheoesophageal fistula. Eur J Hum Genet. 2016; 24(12):1715–23. https://doi.org/10.1038/ejhg.2016.86 PMID: 27436264

27. Zhang R, Marsch F, Kause F, Degenhardt F, Schmiedeke E, Marzheuser S, et al. Array-based molecular karyotyping in 115 VATER/VACTERL and VATER/VACTERL-like patients identifies disease-causing copy number variations. Birth defects research. 2017; 109(13):1063–9. https://doi.org/10.1002/bdr2.1042 PMID: 28605140

28. Veenma D, Brosens E, de Jong E, van de Ven C, Meeussen C, Cohen-Overbeek T, et al. Copy number detection in discordant monozygotic twins of Congenital Diaphragmatic Hernia (CDH) and Esophageal Atresia (EA) cohorts. Eur J Hum Genet. 2012; 20(3):298–304. https://doi.org/10.1038/ejhg.2011.194 PMID: 22071887

29. Gordon CT, Petit F, Oufadem M, Decaestecker C, Jourdain AS, Andrieux J, et al. EFTUD2 haploinsufficiency leads to syndromic oesophageal atresia. J Med Genet. 2012; 49(12):737–46. https://doi.org/10.1136/jmedgenet-2012-101173 PMID: 23188108

30. Lines MA, Huang L, Schwartzentruber J, Douglas SL, Lynch DC, Beaulieu C, et al. Haploinsufficiency of a spliceosomal GTPase encoded by EFTUD2 causes mandibulofacial dysostosis with microcephaly. American journal of human genetics. 2012; 90(2):369–77. https://doi.org/10.1016/j.ajhg.2011.12.023 PMID: 22305528

31. Narchi H. Oesophageal atresia, VACTERL association: Fanconi's anaemia related spectrum of anomalies. Arch Dis Child. 1999; 80(2):207. https://doi.org/10.1136/adc.80.2.207 PMID: 10325745

32. Perel Y, Butenandt O, Carrere A, Saura R, Fayon M, Lamireau T, et al. Oesophageal atresia, VACTERL association: Fanconi's anaemia related spectrum of anomalies. Arch Dis Child. 1998; 78(4):375–6. https://doi.org/10.1136/adc.78.4.375 PMID: 9623406

33. van Bokhoven H, Celli J, van Reeuwijk J, Rinne T, Glaudemans B, van Beusekom E, et al. MYCN haploinsufficiency is associated with reduced brain size and intestinal atresias in Feingold syndrome. Nat Genet. 2005; 37(5):465–7. https://doi.org/10.1038/ng1546 PMID: 15821734

34. Celli J, van Beusekom E, Hennekam RC, Gallardo ME, Smeets DF, de Cordoba SR, et al. Familial syndromic esophageal atresia maps to 2p23-p24. American journal of human genetics. 2000; 66(2):436–44. https://doi.org/10.1086/302779 PMID: 10677303

35. Vissers LE, van Ravenswaaij CM, Admiraal R, Hurst JA, de Vries BB, Janssen IM, et al. Mutations in a new member of the chromodomain gene family cause CHARGE syndrome. Nat Genet. 2004; 36(9):955–7. https://doi.org/10.1038/ng1407 PMID: 15300250

36. Jongmans MC, Admiraal RJ, van der Donk KP, Vissers LE, Baas AF, Kapusta L, et al. CHARGE syndrome: the phenotypic spectrum of mutations in the CHD7 gene. J Med Genet. 2006; 43(4):306–14. https://doi.org/10.1136/jmg.2005.036061 PMID: 16155193

37. Williamson KA, Hever AM, Rainger J, Rogers RC, Magee A, Fiedler Z, et al. Mutations in SOX2 cause anophthalmia-esophageal-genital (AEG) syndrome. Hum Mol Genet. 2006; 15(9):1413–22. https://doi.org/10.1093/hmg/ddl064 PMID: 16543359

38. Pinson L, Auge J, Audollent S, Mattei G, Etchevers H, Gigarel N, et al. Embryonic expression of the human MID1 gene and its mutations in Opitz syndrome. J Med Genet. 2004; 41(5):381–6. https://doi.org/10.1136/jmg.2003.014829 PMID: 15121778

39. De Falco F, Cainarca S, Andolfi G, Ferrentino R, Berti C, Rodriguez Criado G, et al. X-linked Opitz syndrome: novel mutations in the MID1 gene and redefinition of the clinical spectrum. Am J Med Genet A. 2003; 120(2):222–8. https://doi.org/10.1002/ajmg.a.10265 PMID: 12833403

40. Mnayer L, Khuri S, Merheby HA, Meroni G, Elsas LJ. A structure-function study of MID1 mutations associated with a mild Opitz phenotype. Mol Genet Metab. 2006; 87(3):198–203. https://doi.org/10.1016/j.ymgme.2005.10.014 PMID: 16378742

41. Sakiyama J, Yamagishi A, Kuroiwa A. Tbx4-Fgf10 system controls lung bud formation during chicken embryonic development. Development (Cambridge, England). 2003; 130(7):1225–34. https://doi.org/10.1242/dev.00345 PMID: 12588840

42. Li S, Zhou D, Lu MM, Morrisey EE. Advanced cardiac morphogenesis does not require heart tube fusion. Science (New York, NY). 2004; 305(5690):1619–22.

43. Mahlapuu M, Enerback S, Carlsson P. Haploinsufficiency of the forkhead gene Foxf1, a target for sonic hedgehog signaling, causes lung and foregut malformations. Development (Cambridge, England). 2001; 128(12):2397–406. PMID: 11493558

44. Shu W, Lu MM, Zhang Y, Tucker PW, Zhou D, Morrisey EE. Foxp2 and Foxp1 cooperatively regulate lung and esophagus development. Development (Cambridge, England). 2007; 134(10):1991–2000. https://doi.org/10.1242/dev.02846 PMID: 17428829

45. Ya J, Schilham MW, de Boer PA, Moorman AF, Clevers H, Lamers WH. Sox4-deficiency syndrome in mice is an animal model for common trunk. Circulation research. 1998; 83(10):986–94. https://doi.org/10.1161/01.res.83.10.986 PMID: 9815146

46. Que J, Okubo T, Goldenring JR, Nam KT, Kurotani R, Morrisey EE, et al. Multiple dose-dependent roles for Sox2 in the patterning and differentiation of anterior foregut endoderm. Development (Cambridge, England). 2007; 134(13):2521–31. https://doi.org/10.1242/dev.003855 PMID: 17522155

47. Bachiller D, Klingensmith J, Kemp C, Belo JA, Anderson RM, May SR, et al. The organizer factors Chordin and Noggin are required for mouse forebrain development. Nature. 2000; 403(6770):658–61. https://doi.org/10.1038/35001072 PMID: 10688202

48. Bachiller D, Klingensmith J, Shneyder N, Tran U, Anderson R, Rossant J, et al. The role of chordin/Bmp signals in mammalian pharyngeal development and DiGeorge syndrome. Development (Cambridge, England). 2003; 130(15):3567–78. https://doi.org/10.1242/dev.00581 PMID: 12810603

49. Que J, Choi M, Ziel JW, Klingensmith J, Hogan BL. Morphogenesis of the trachea and esophagus: current players and new roles for noggin and Bmps. Differentiation. 2006; 74(7):422–37. https://doi.org/10.1111/j.1432-0436.2006.00096.x PMID: 16916379

50. Li Y, Litingtung Y, Ten Dijke P, Chiang C. Aberrant Bmp signaling and notochord delamination in the pathogenesis of esophageal atresia. Developmental dynamics: an official publication of the American Association of Anatomists. 2007; 236(3):746–54. https://doi.org/10.1002/dvdy.21075 PMID: 17260385

51. Li Y, Gordon J, Manley NR, Litingtung Y, Chiang C. Bmp4 is required for tracheal formation: a novel mouse model for tracheal agenesis. Developmental biology. 2008; 322(1):145–55. https://doi.org/10.1016/j.ydbio.2008.07.021 PMID: 18692041

52. Miller LA, Wert SE, Clark JC, Xu Y, Perl AK, Whitsett JA. Role of Sonic hedgehog in patterning of tracheal-bronchial cartilage and the peripheral lung. Developmental dynamics: an official publication of the American Association of Anatomists. 2004; 231(1):57–71. https://doi.org/10.1002/dvdy.20105 PMID: 15305287

53. Pepicelli CV, Lewis PM, McMahon AP. Sonic hedgehog regulates branching morphogenesis in the mammalian lung. Current biology: CB. 1998; 8(19):1083–6. https://doi.org/10.1016/s0960-9822(98)70446-4 PMID: 9768363

54. Litingtung Y, Lei L, Westphal H, Chiang C. Sonic hedgehog is essential to foregut development. Nat Genet. 1998; 20(1):58–61. https://doi.org/10.1038/1717 PMID: 9731532

55. Motoyama J, Liu J, Mo R, Ding Q, Post M, Hui CC. Essential function of Gli2 and Gli3 in the formation of lung, trachea and oesophagus. Nat Genet. 1998; 20(1):54–7. https://doi.org/10.1038/1711 PMID: 9731531

56. Friedland-Little JM, Hoffmann AD, Ocbina PJ, Peterson MA, Bosman JD, Chen Y, et al. A novel murine allele of Intraflagellar Transport Protein 172 causes a syndrome including VACTERL-like features with hydrocephalus. Hum Mol Genet. 2011; 20(19):3725–37. https://doi.org/10.1093/hmg/ddr241 PMID: 21653639

57. Mill P, Lockhart PJ, Fitzpatrick E, Mountford HS, Hall EA, Reijns MA, et al. Human and mouse mutations in WDR35 cause short-rib polydactyly syndromes due to abnormal ciliogenesis. American journal of human genetics. 2011; 88(4):508–15. https://doi.org/10.1016/j.ajhg.2011.03.015 PMID: 21473986

58. Kaltman JR, Schramm C, Pearson GD. The National Heart, Lung, and Blood Institute bench to bassinet Program: a new paradigm for translational research. Journal of the American College of Cardiology. 2010; 55(12):1262–5. https://doi.org/10.1016/j.jacc.2009.11.055 PMID: 20298934

59. Nam KT, Lee HJ, Smith JJ, Lapierre LA, Kamath VP, Chen X, et al. Loss of Rab25 promotes the development of intestinal neoplasia in mice and is associated with human colorectal adenocarcinomas. The Journal of clinical investigation. 2010; 120(3):840–9. https://doi.org/10.1172/JCI40728 PMID: 20197623

60. Garber ED. "Bent-Tail," A Dominant, Sex-Linked Mutation in the Mouse. Proceedings of the National Academy of Sciences of the United States of America. 1952; 38(10):876–9. https://doi.org/10.1073/pnas.38.10.876 PMID: 16589192

61. Hu Y, Baud V, Delhase M, Zhang P, Deerinck T, Ellisman M, et al. Abnormal morphogenesis but intact IKK activation in mice lacking the IKKalpha subunit of IkappaB kinase. Science (New York, NY). 1999; 284(5412):316–20. https://doi.org/10.1126/science.284.5412.316 PMID: 10195896

62. Goss AM, Tian Y, Tsukiyama T, Cohen ED, Zhou D, Lu MM, et al. Wnt2/2b and beta-catenin signaling are necessary and sufficient to specify lung progenitors in the foregut. Developmental cell. 2009; 17 (2):290–8. https://doi.org/10.1016/j.devcel.2009.06.005 PMID: 19686689

63. Holland P, Willis C, Kanaly S, Glaccum M, Warren A, Charrier K, et al. RIP4 is an ankyrin repeat-containing kinase essential for keratinocyte differentiation. Current biology: CB. 2002; 12(16):1424–8. https://doi.org/10.1016/s0960-9822(02)01075-8 PMID: 12194825

64. Brosens E, Ploeg M, van Bever Y, Koopmans AE, H IJ, Rottier RJ, et al. Clinical and etiological heterogeneity in patients with tracheo-esophageal malformations and associated anomalies. European journal of medical genetics. 2014. https://doi.org/10.1016/j.ejmg.2014.05.009 PMID: 24931924

65. Moore KL. Respiratory system. In: Moore KL, editor. Essentials of human embryology. Philadelphia: B.C.Decker Inc; 1988. p. 91.

66. Zaw-Tun HA. The tracheo-esophageal septum—fact or fantasy? Origin and development of the respiratory primordium and esophagus. Acta Anat (Basel). 1982; 114(1):1–21. PMID: 7148374

67. Kluth D, Fiegel H. The embryology of the foregut. Semin Pediatr Surg. 2003; 12(1):3–9. https://doi.org/10.1053/spsu.2003.50003 PMID: 12520468

68. Qi BQ, Beasley SW. Stages of normal tracheo-bronchial development in rat embryos: resolution of a controversy. Dev Growth Differ. 2000; 42(2):145–53. https://doi.org/10.1046/j.1440-169x.2000.00488.x PMID: 10830438

69. Kluth D, Steding G, Seidl W. The embryology of foregut malformations. J Pediatr Surg. 1987; 22 (5):389–93. https://doi.org/10.1016/s0022-3468(87)80254-3 PMID: 3585660

70. Merei JM, Hutson JM. Embryogenesis of tracheo esophageal anomalies: a review. Pediatr Surg Int. 2002; 18(5–6):319–26. https://doi.org/10.1007/s00383-002-0751-1 PMID: 12415347

71. Crisera CA, Connelly PR, Marmureanu AR, Colen KL, Rose MI, Li M, et al. Esophageal atresia with tracheoesophageal fistula: suggested mechanism in faulty organogenesis. J Pediatr Surg. 1999; 34 (1):204–8. https://doi.org/10.1016/s0022-3468(99)90258-0 PMID: 10022173

72. Spilde TL, Bhatia AM, Marosky JK, Hembree MJ, Kobayashi H, Daume EL, et al. Complete discontinuity of the distal fistula tract from the developing gut: direct histologic evidence for the mechanism of tracheoesophageal fistula formation. The Anatomical record. 2002; 267(3):220–4. https://doi.org/10.1002/ar.10106 PMID: 12115271

73. Spilde T, Bhatia A, Ostlie D, Marosky J, Holcomb G 3rd, Snyder C, et al. A role for sonic hedgehog signaling in the pathogenesis of human tracheoesophageal fistula. J Pediatr Surg. 2003; 38(3):465–8. https://doi.org/10.1053/jpsu.2003.50080 PMID: 12632368

74. Spilde TL, Bhatia AM, Miller KA, Ostlie DJ, Chaignaud BE, Holcomb GW 3rd, et al. Thyroid transcription factor-1 expression in the human neonatal tracheoesophageal fistula. J Pediatr Surg. 2002; 37 (7):1065–7. https://doi.org/10.1053/jpsu.2002.33845 PMID: 12077772

75. Crowley AR, Mehta SS, Hembree MJ, Preuett BL, Prasadan KL, Sharp SW, et al. Bone morphogenetic protein expression patterns in human esophageal atresia with tracheoesophageal fistula. Pediatr Surg Int. 2006; 22(2):154–7. https://doi.org/10.1007/s00383-005-1598-z PMID: 16315037

76. Dutta HK, Mathur M, Bhatnagar V. A histopathological study of esophageal atresia and tracheoesophageal fistula. J Pediatr Surg. 2000; 35(3):438–41. https://doi.org/10.1016/s0022-3468(00)90209-4 PMID: 10726684

77. Hokama NA M, M K, PE C, CW C. Esophagel atresia with tracheo-esophageal fistula. A histopathological study. Pediatr Surg Int. 1986; 1:117–21.

78. Crisera CA, Connelly PR, Marmureanu AR, Li M, Rose MI, Longaker MT, et al. TTF-1 and HNF-3beta in the developing tracheoesophageal fistula: further evidence for the respiratory origin of the distal

esophagus. J Pediatr Surg. 1999; 34(9):1322–6. https://doi.org/10.1016/s0022-3468(99)90003-9 PMID: 10507421

79. Crisera CA, Maldonado TS, Kadison AS, Li M, Longaker MT, Gittes GK. Patterning of the "distal esophagus" in esophageal atresia with tracheo- esophageal fistula: is thyroid transcription factor 1 a player? J Surg Res. 2000; 92(2):245–9. https://doi.org/10.1006/jsre.2000.5850 PMID: 10896829

80. Ioannides AS, Chaudhry B, Henderson DJ, Spitz L, Copp AJ. Dorsoventral patterning in oesophageal atresia with tracheo-oesophageal fistula: Evidence from a new mouse model. J Pediatr Surg. 2002; 37 (2):185–91. https://doi.org/10.1053/jpsu.2002.30252 PMID: 11819196

81. Smigiel R, Lebioda A, Blaszczynski M, Korecka K, Czauderna P, Korlacki W, et al. Alternations in genes expression of pathway signaling in esophageal tissue with atresia: results of expression microarray profiling. Diseases of the esophagus: official journal of the International Society for Diseases of the Esophagus. 2015; 28(3):229–33. https://doi.org/10.1111/dote.12173 PMID: 24460849

82. van de Putte R, Dworschak GC, Brosens E, Reutter HM, Marcelis CLM, Acuna-Hidalgo R, et al. A Genetics-First Approach Revealed Monogenic Disorders in Patients With ARM and VACTERL Anomalies. Frontiers in pediatrics. 2020; 8:310. https://doi.org/10.3389/fped.2020.00310 PMID: 32656166

83. Sherwood RI, Chen TY, Melton DA. Transcriptional dynamics of endodermal organ formation. Developmental dynamics: an official publication of the American Association of Anatomists. 2009; 238 (1):29–42. https://doi.org/10.1002/dvdy.21810 PMID: 19097184

84. Millien G, Beane J, Lenburg M, Tsao PN, Lu J, Spira A, et al. Characterization of the mid-foregut transcriptome identifies genes regulated during lung bud induction. Gene expression patterns: GEP. 2008; 8(2):124–39. https://doi.org/10.1016/j.modgep.2007.09.003 PMID: 18023262

85. Solomon BD, Bear KA, Kimonis V, de Klein A, Scott DA, Shaw-Smith C, et al. Clinical geneticists' views of VACTERL/VATER association. Am J Med Genet A. 2012; 158a(12):3087–100. https://doi.org/10.1002/ajmg.a.35638 PMID: 23165726

86. Wallace AS, Burns AJ. Development of the enteric nervous system, smooth muscle and interstitial cells of Cajal in the human gastrointestinal tract. Cell Tissue Res. 2005; 319(3):367–82. https://doi.org/10.1007/s00441-004-1023-2 PMID: 15672264

87. Rao M, Gershon MD. Enteric nervous system development: what could possibly go wrong? Nat Rev Neurosci. 2018; 19(9):552–65. https://doi.org/10.1038/s41583-018-0041-0 PMID: 30046054

88. Rodriguez P, Da Silva S, Oxburgh L, Wang F, Hogan BL, Que J. BMP signaling in the development of the mouse esophagus and forestomach. Development (Cambridge, England). 2010; 137(24):4171–6. https://doi.org/10.1242/dev.056077 PMID: 21068065

89. Jacobs IJ, Que J. Genetic and cellular mechanisms of the formation of esophageal atresia and tracheoesophageal fistula. Diseases of the esophagus: official journal of the International Society for Diseases of the Esophagus. 2013; 26(4):356–8. https://doi.org/10.1111/dote.12055 PMID: 23679023

90. Dravis C, Henkemeyer M. Ephrin-B reverse signaling controls septation events at the embryonic midline through separate tyrosine phosphorylation-independent signaling avenues. Developmental biology. 2011; 355(1):138–51. https://doi.org/10.1016/j.ydbio.2011.04.020 PMID: 21539827

91. Yamada KM, Miyamoto S. Integrin transmembrane signaling and cytoskeletal control. Current opinion in cell biology. 1995; 7(5):681–9. https://doi.org/10.1016/0955-0674(95)80110-3 PMID: 8573343

92. Humphrey JD, Dufresne ER, Schwartz MA. Mechanotransduction and extracellular matrix homeostasis. Nature reviews Molecular cell biology. 2014; 15(12):802–12. https://doi.org/10.1038/nrm3896 PMID: 25355505

93. Liu S, Calderwood DA, Ginsberg MH. Integrin cytoplasmic domain-binding proteins. Journal of Cell Science. 2000; 113(20):3563–71. PMID: 11017872

94. Turner CE. Paxillin and focal adhesion signalling. Nature cell biology. 2000; 2(12):E231–6. https://doi.org/10.1038/35046659 PMID: 11146675

95. Hagel M, George EL, Kim A, Tamimi R, Opitz SL, Turner CE, et al. The Adaptor Protein Paxillin Is Essential for Normal Development in the Mouse and Is a Critical Transducer of Fibronectin Signaling. Molecular and Cellular Biology. 2002; 22(3):901–15. https://doi.org/10.1128/mcb.22.3.901-915.2002 PMID: 11784865

96. Zhang Z, Rankin SA, Zorn AM. Syndecan4 coordinates Wnt/JNK and BMP signaling to regulate foregut progenitor development. Developmental biology. 2016; 416(1):187–99. https://doi.org/10.1016/j.ydbio.2016.05.025 PMID: 27235146

97. Villegas SN, Canham M, Brickman JM. FGF signalling as a mediator of lineage transitions—evidence from embryonic stem cell differentiation. Journal of cellular biochemistry. 2010; 110(1):10–20. https://doi.org/10.1002/jcb.22536 PMID: 20336694

98. Villegas SN, Rothova M, Barrios-Llerena ME, Pulina M, Hadjantonakis AK, Le Bihan T, et al. PI3K/Akt1 signalling specifies foregut precursors by generating regionalized extra-cellular matrix. eLife. 2013; 2:e00806. https://doi.org/10.7554/eLife.00806 PMID: 24368729

99. Philpott A, Porro EB, Kirschner MW, Tsai LH. The role of cyclin-dependent kinase 5 and a novel regulatory subunit in regulating muscle differentiation and patterning. Genes & development. 1997; 11 (11):1409–21. https://doi.org/10.1101/gad.11.11.1409 PMID: 9192869

100. Humbert S, Dhavan R, Tsai L. p39 activates cdk5 in neurons, and is associated with the actin cytoskeleton. J Cell Sci. 2000; 113 (Pt 6):975–83.

101. He L, Zhang Z, Yu Y, Ahmed S, Cheung NS, Qi RZ. The neuronal p35 activator of Cdk5 is a novel F-actin binding and bundling protein. Cellular and molecular life sciences: CMLS. 2011; 68(9):1633–43. https://doi.org/10.1007/s00018-010-0562-9 PMID: 20976519

102. Xu J, Tsutsumi K, Tokuraku K, Estes KA, Hisanaga S, Ikezu T. Actin interaction and regulation of cyclin-dependent kinase 5/p35 complex activity. Journal of neurochemistry. 2011; 116(2):192–204. https://doi.org/10.1111/j.1471-4159.2010.06824.x PMID: 20492361

103. Ryan GB, Cliff WJ, Gabbiani G, Irle C, Montandon D, Statkov PR, et al. Myofibroblasts in human granulation tissue. Human pathology. 1974; 5(1):55–67. https://doi.org/10.1016/s0046-8177(74)80100-0 PMID: 4588257

104. Stempien-Otero A, Kim DH, Davis J. Molecular networks underlying myofibroblast fate and fibrosis. Journal of molecular and cellular cardiology. 2016; 97:153–61. https://doi.org/10.1016/j.yjmcc.2016.05.002 PMID: 27167848

105. Chambers RC, Leoni P, Kaminski N, Laurent GJ, Heller RA. Global expression profiling of fibroblast responses to transforming growth factor-beta1 reveals the induction of inhibitor of differentiation-1 and provides evidence of smooth muscle cell phenotypic switching. The American journal of pathology. 2003; 162(2):533–46. https://doi.org/10.1016/s0002-9440(10)63847-3 PMID: 12547711

106. Malmstrom J, Lindberg H, Lindberg C, Bratt C, Wieslander E, Delander EL, et al. Transforming growth factor-beta 1 specifically induce proteins involved in the myofibroblast contractile apparatus. Molecular & cellular proteomics: MCP. 2004; 3(5):466–77. https://doi.org/10.1074/mcp.M300108-MCP200 PMID: 14766930

107. Untergasser G, Gander R, Lilg C, Lepperdinger G, Plas E, Berger P. Profiling molecular targets of TGF-beta1 in prostate fibroblast-to-myofibroblast transdifferentiation. Mechanisms of ageing and development. 2005; 126(1):59–69. https://doi.org/10.1016/j.mad.2004.09.023 PMID: 15610763

108. Kapoun AM, Gaspar NJ, Wang Y, Damm D, Liu YW, O'Young G, et al. Transforming growth factor-beta receptor type 1 (TGFbetaRI) kinase activity but not p38 activation is required for TGFbetaRI-induced myofibroblast differentiation and profibrotic gene expression. Molecular pharmacology. 2006; 70(2):518–31. https://doi.org/10.1124/mol.105.021600 PMID: 16707625

109. Mori Y, Ishida W, Bhattacharyya S, Li Y, Platanias LC, Varga J. Selective inhibition of activin receptor-like kinase 5 signaling blocks profibrotic transforming growth factor beta responses in skin fibroblasts. Arthritis and rheumatism. 2004; 50(12):4008–21. https://doi.org/10.1002/art.20658 PMID: 15593186

110. Thomas M, Docx C, Holmes AM, Beach S, Duggan N, England K, et al. Activin-like kinase 5 (ALK5) mediates abnormal proliferation of vascular smooth muscle cells from patients with familial pulmonary arterial hypertension and is involved in the progression of experimental pulmonary arterial hypertension induced by monocrotaline. The American journal of pathology. 2009; 174(2):380–9. https://doi.org/10.2353/ajpath.2009.080565 PMID: 19116361

111. Minoo P, Su G, Drum H, Bringas P, Kimura S. Defects in tracheoesophageal and lung morphogenesis in Nkx2.1(-/-) mouse embryos. Developmental biology. 1999; 209(1):60–71. https://doi.org/10.1006/dbio.1999.9234 PMID: 10208743

112. Baltus GA, Kowalski MP, Zhai H, Tutter AV, Quinn D, Wall D, et al. Acetylation of sox2 induces its nuclear export in embryonic stem cells. Stem cells (Dayton, Ohio). 2009; 27(9):2175–84. https://doi.org/10.1002/stem.168 PMID: 19591226

113. Ishii Y, Rex M, Scotting PJ, Yasugi S. Region-specific expression of chicken Sox2 in the developing gut and lung epithelium: regulation by epithelial-mesenchymal interactions. Developmental dynamics: an official publication of the American Association of Anatomists. 1998; 213(4):464–75. https://doi.org/10.1002/(SICI)1097-0177(199812)213:4<464::AID-AJA11>3.0.CO;2-Z PMID: 9853967

114. Li Y, Litingtung Y, Ten Dijke P, Chiang C. Aberrant Bmp signaling and notochord delamination in the pathogenesis of esophageal atresia. Dev Dyn. 2007. https://doi.org/10.1002/dvdy.21075 PMID: 17260385

115. Gontan C, de Munck A, Vermeij M, Grosveld F, Tibboel D, Rottier R. Sox2 is important for two crucial processes in lung development: branching morphogenesis and epithelial cell differentiation. Developmental biology. 2008; 317(1):296–309. https://doi.org/10.1016/j.ydbio.2008.02.035 PMID: 18374910

116. Nagy N, Goldstein AM. Enteric nervous system development: A crest cell's journey from neural tube to colon. Seminars in cell & developmental biology. 2017; 66:94–106.

117. Kishimoto K, Tamura M, Nishita M, Minami Y, Yamaoka A, Abe T, et al. Synchronized mesenchymal cell polarization and differentiation shape the formation of the murine trachea and esophagus. Nat Commun. 2018; 9(1):2816. https://doi.org/10.1038/s41467-018-05189-2 PMID: 30026494

118. Mazzone SB, McGovern AE. Innervation of tracheal parasympathetic ganglia by esophageal cholinergic neurons: evidence from anatomic and functional studies in guinea pigs. American journal of physiology Lung cellular and molecular physiology. 2010; 298(3):L404–16. https://doi.org/10.1152/ajplung.00166.2009 PMID: 20061441

119. Yu WY, Slack JM, Tosh D. Conversion of columnar to stratified squamous epithelium in the developing mouse oesophagus. Developmental biology. 2005; 284(1):157–70. https://doi.org/10.1016/j.ydbio.2005.04.042 PMID: 15992795

120. DeWard AD, Cramer J, Lagasse E. Cellular heterogeneity in the mouse esophagus implicates the presence of a nonquiescent epithelial stem cell population. Cell reports. 2014; 9(2):701–11. https://doi.org/10.1016/j.celrep.2014.09.027 PMID: 25373907

121. Daniely Y, Liao G, Dixon D, Linnoila RI, Lori A, Randell SH, et al. Critical role of p63 in the development of a normal esophageal and tracheobronchial epithelium. American journal of physiology Cell physiology. 2004; 287(1):C171–81. https://doi.org/10.1152/ajpcell.00226.2003 PMID: 15189821

122. Moll R, Franke WW, Schiller DL, Geiger B, Krepler R. The catalog of human cytokeratins: patterns of expression in normal epithelia, tumors and cultured cells. Cell. 1982; 31(1):11–24. https://doi.org/10.1016/0092-8674(82)90400-7 PMID: 6186379

123. Li K, Zheng S, Xiao X, Wang Q, Zhou Y, Chen L. The structural characteristics and expression of neuropeptides in the esophagus of patients with congenital esophageal atresia and tracheoesophageal fistula. J Pediatr Surg. 2007; 42(8):1433–8. https://doi.org/10.1016/j.jpedsurg.2007.03.050 PMID: 17706510